Ground Support 2026 - D Cumming-Potvin & J Wesseloo (eds.)
© 2026 Australian Centre for Geomechanics, Perth
doi:10.36487/ACG_repo/2625_48

Operational assessment of dynamic demand imposed on ground support during large seismic events

Dmitriy Malovichko [a,*], Alex Rigby [a], Stefan Mroczek [a]

[a] *Institute of Mine Seismology, Australia*

Abstract

Large seismic events recorded in mines often exhibit complex waveforms, indicating that rock mass failure and the associated deformation of excavations evolve dynamically in space and time. It is of practical importance to infer the characteristics of this evolution from the recorded waveforms, as this enables the quantification of the dynamic demand imposed on ground support (e.g. in terms of tunnel surface displacement or kinetic energy). Detailed reconstruction of spatio-temporal characteristics of seismic sources is possible (Malovichko et al. 2025); however, it requires significant effort and is not feasible in an operational context (e.g. within a few hours after an event).

For seismic events associated with sudden slip along a planar surface or shear failure in a confined environment, the strongest near-source peak ground velocity can be estimated using the relatively simple method proposed by McGarr (1991). By combining this estimate with conservative assumptions about source spatial distribution, maps of peak ground velocity for the tunnels can be constructed. However, this method cannot be applied to events involving episodes of excavation convergence and the paper proposes an approach to address this limitation. The rapid evaluation of strainburst demand parameters (e.g. strainburst depth, bulking velocity) is possible assuming that the strongest far-field displacement pulses are associated with the most severe episode of dynamic stress fracturing at the tunnel/s perimeter. The subsequent mapping of the demand parameters is then presented.

The proposed approach is demonstrated using real data from two mines. Its application to operational rockburst damage forecasting is illustrated.

Keywords: *rockburst, seismicity, seismic source*

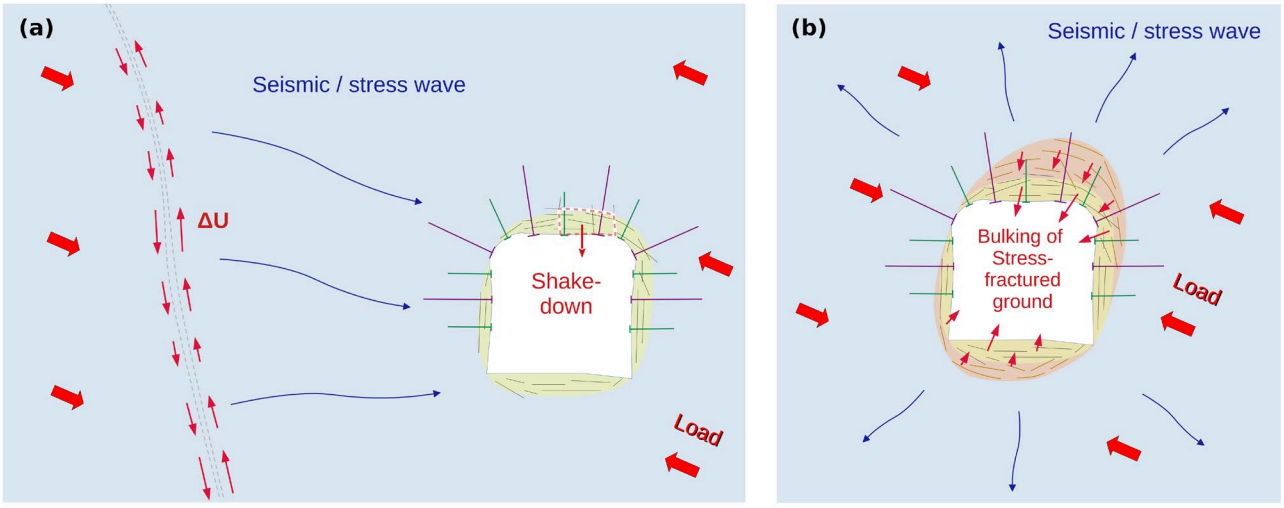
1 Introduction

When analysing rockburst damage in mines, it is beneficial to consider the 2 mechanisms of demand imposed on ground support presented by Kaiser et al. (1996):

- The first mechanism is driven by strong ground motion associated with seismic waves radiated by an external dynamic failure process. In Figure 1a, this external process is represented by shear failure, or slip, along a geological structure. However, other types of distant seismic sources are also possible, such as pillar failure. Regardless of the seismic source type, the dynamic demand is controlled by the characteristics of the ground motion at the tunnel location, particularly its intensity. As shown by Rigby et al. (2026c), peak ground velocity (PGV) is one of the best predictors of the consumed displacement capacity of rockbolts among the various ground motion intensity measures used in earthquake engineering (e.g. peak ground acceleration, cumulative absolute velocity or displacement, etc.).
- The second mechanism, illustrated in Figure 1b, comprises the dynamic bulking of stress-fractured rock at the tunnel perimeter. This process, together with the associated rapid convergence of the

* Corresponding author. Email address: dima@imsi.org

surrounding rock mass, radiates seismic waves and is often registered as a seismic event with a crush-type mechanism. The magnitude of such an event can be significant if multiple tunnels are involved (e.g. in a cascading tunnel damage scenario). Unlike the previous case, the demand imposed on the ground support is not defined by the intensity of the radiated seismic waves. Instead, it is controlled by the amount and rate of bulking of the stress-fractured rock, characterised by the strainburst depth (d_{SB}) and the strainburst (or bulking) velocity (V_{SB}).



(a) (b)

Figure 1 Two types of seismic events and the corresponding rockburst damage mechanisms. Rock that was damaged prior to the seismic event is shown in yellow; (a) Dynamic impact in the form of seismic waves from an external seismic event, causing shakedown damage; (b) In the strainburst case, the rock undergoing dynamic fracturing and bulking is shown in red

Therefore, for the seismic shakedown damage mechanism, it is appropriate to evaluate PGV at the tunnel locations, whereas for strainbursting, maps of d_{SB} and V_{SB} are required.

The forecasting of demand in the form of PGV, d_{SB}, and V_{SB} for future mining, and its comparison with the remnant capacity of the installed or planned ground support, are discussed in other publications (Kaiser & Malovichko 2022; Malovichko et al. 2024; Rigby et al. 2026a). The focus of this paper is on retrospective assessment, specifically situations in which a significant seismic event has occurred in a mine and it is critical to rapidly estimate the affected area and the likelihood of damage. Such an assessment should be completed as quickly as possible, ideally within one hour of the event.

For moderate-sized seismic events with simple waveforms comprising distinct, isolated P-wave and S-wave pulses, the seismic radiation can be approximated by a point source, making the demand evaluation relatively straightforward:

- A PGV map can be generated using a ground motion prediction equation (GMPE), preferably calibrated for the mine. The GMPE takes as input the source parameters (e.g. scalar seismic moment or potency, or seismic energy) together with the distance to the source location, preferably accounting for its uncertainty.
- The d_{SB} can be inferred from the scalar moment of a crush-type event associated with a tunnel. Measuring the bulking duration from the waveforms (Malovichko 2022), together with an assumed bulking factor (BF), allows d_{SB} to be converted into the V_{SB}. The resulting d_{SB} and V_{SB} values can then be plotted on the mine plans based on the estimated source location, while accounting for its uncertainty.

The assessment is more challenging for large seismic events with complex waveforms as in examples presented in Figure 2. In such cases, the seismic event location (which typically represents the point of

failure initiation) may not correspond to the location of the highest demand. The later high-amplitude pulses in the recorded waveforms (as illustrated in Figure 2) may correspond to intense episodes of failure occurring at locations far from the point of failure initiation. Another challenge is that the source parameters (e.g. seismic moment and seismic energy) characterise the source as a whole. Consequently, the parameters derived from them (e.g. stress drop and the corresponding PGV) effectively smear out localised high-energy failure episodes that may impose significant demand on the ground support.

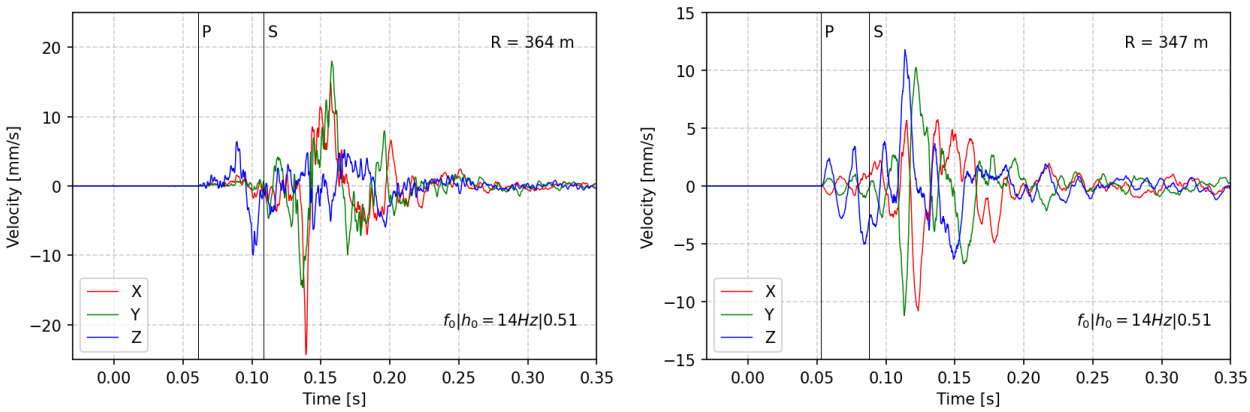


Figure 2 Examples of velocity waveforms from complex seismic events. The multiple signals are not related to the medium heterogeneity. Instead, they result from the complex spatio-temporal pattern of rock mass failure

The reconstruction of the spatio-temporal characteristics of complex seismic sources and their translation into ground support demand parameters are possible, as discussed by Malovichko et al. (2025). However, the underlying finite-source inversion procedure is computationally demanding and currently requires at least a few days to complete. In this paper, we propose an express procedure for generating maps of the demand parameters (PGV, d_{SB}, and V_{SB}), which can be applied within one hour of the occurrence of a large seismic event. The procedure is based on conservative approximations that may lead to an overestimation of the demand. Such conservatism is justified in an operational context, as a more accurate assessment based on finite-source inversion can be undertaken later, if required, once additional information becomes available (e.g. aftershocks and underground observations).

The proposed method is summarised in Section 2. The subsequent sections demonstrate its application to 2 large seismic events representing slip- and crush-type source mechanisms. The paper concludes with a discussion of the method's applications, limitations and directions for future work.

2 Method

A method to assess the near-fault peak ground velocity is suggested by McGarr (1991). It is based on the assumption that the strongest near-source ground motion is associated with the rupture of a smaller part of the source (asperity), which produces the most intensive velocity pulse in far-field waveforms. In an illustrative example shown in Figure 3, the total far-field velocity waveform (red) consists of the superposition of pulses from asperities 1 and 2 (blue and green, respectively), as well as radiation from the remaining parts of the fault r_0. The strongest far-field ground motion velocity is associated with the pulse from asperity 2.

The maximum slip velocity, $\dot{D}$, is evaluated as follows:

$$\dot{D} = 2.56(\beta/\mu)\rho R a \tag{1}$$

where:

a = peak ground acceleration associated with strongest velocity pulse

β = velocity of S-waves

μ = shear modulus

ρ = rock mass density

R = hypocentral distance.

The strongest near-source ground velocity (in the vicinity of the asperity 2 in the example above) will be $\dot{\mathrm{D}}/2$.

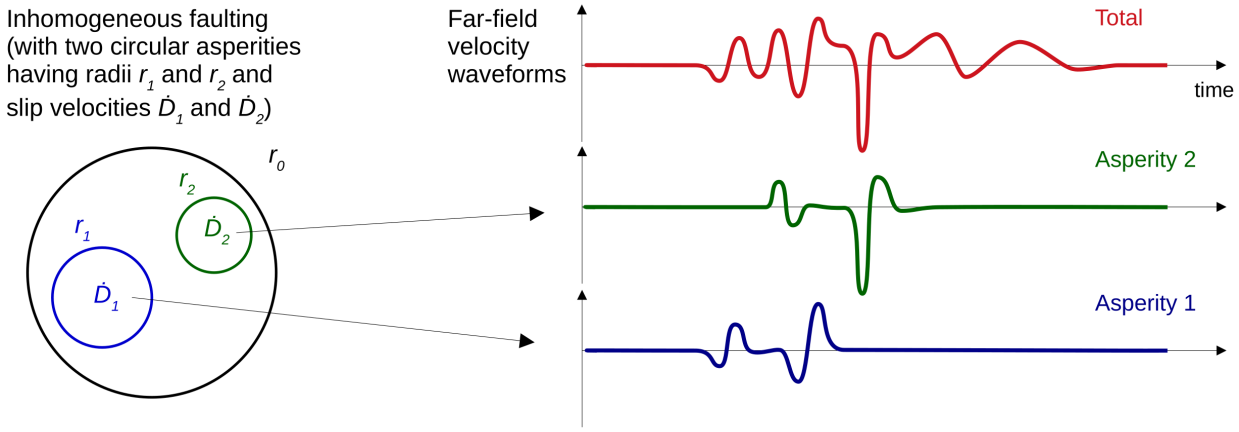


Figure 3 A schematic source model of inhomogeneous faulting, adapted from McGarr (1991). $\dot{\mathrm{D}}$ = maximum slip velocity

The method of McGarr (1991) allows the maximum intensity of ground motion to be assessed; however, it does not indicate where this maximum occurred in space. To create a map of the plausible dynamic demand associated with a particular complex event, we propose a procedure consisting of the following steps:

- Establish the spatial distribution of the source and approximate it using one or more ellipsoids. The following information can be used: the location of the source initiation (including its uncertainty), the source mechanism (e.g. the orientation of the nodal planes), the source dimensions inferred from the corner frequency, and the spatial distribution and mechanisms of aftershocks.
- Use a GMPE in the functional form proposed by Mendecki (2019), preferably calibrated for the mine. Adjust the near-source term so that the inferred maximum PGV matches the value estimated using the method of McGarr (1991) as described above.
- Calculate the PGV for the tunnels using the adjusted GMPE, the total seismic potency of the event, and distance measure to the established source volume.

This procedure provides a conservative estimate of the dynamic demand because it assumes that the maximum slip velocity occurs throughout the source, rather than being localised. The procedure is relatively simple and can be implemented within an hour after a large event. It is illustrated in the next section using data from a real mine.

The McGarr (1991) method is applicable to slip-type events, i.e. dynamic shear failure or slip along a planar surface occurring in a confined environment that does not involve sudden permanent deformation of excavations. If a large, complex seismic event exhibits a crush-type mechanism, the method is not applicable.

If a recorded crush-type event could be associated with tunnels, then the express assessment of the demand can be done using the same logic as was employed by McGarr (1991). Assuming that the largest displacement pulse within complex waveforms is attributed to a section of particular tunnel (Figure 4), the corresponding d_{SB} can be inferred as described below.

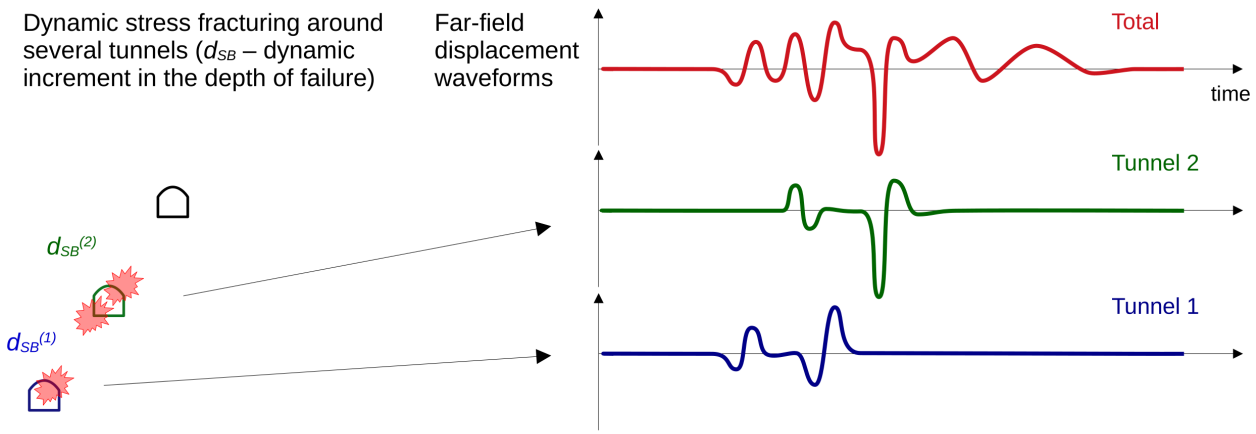


Figure 4 Extension of the McGarr (1991) model to strainbursting at multiple locations. d_{SB} = strainburst depth

The far-field peak displacement pulse in the waveforms, PGD, can be expressed as follows:

$$PGD = [A_{FS}/(4\pi\rho\beta^3 R)]\dot{M}_0^{max} \quad (2)$$

where:

A_{FS} = far-field radiation pattern of S-wave for a closing crack point source model

ρ = rock mass density

β = velocity of S-waves

R = distance from the sensor to possible damage location

$\dot{M}_0^{max} = 2[(1-\nu)/(1-2\nu)]\sigma_{1p} L_d (D + SF\, d_{SB}) SF\, d_{SB}/t_{SB}$ = maximum rate of scalar seismic moment for a dynamic stress fracturing around a tunnel according to model suggested by Malovichko (2022) and Malovichko & Rigby (2022)

ν = Poisson's ratio

σ_{1p} = maximum in-plane stress (plane is orthogonal to the tunnel's axis)

D = effective tunnel diameter

L_d = extent of damage along the runnel

SF = split factor ranging from 1 (failure on one side of the tunnel) to 2 (equal failure on both sides)

d_{SB} = strainburst depth

t_{SB} = strainburst (or bulking) duration, which is evaluated from the duration of the strongest displacement pulse.

The expression can be simplified using the following assumptions:

- ν = 0.25 and, correspondingly, A_{FS} = 0.31
- SF = 1, which makes the assessment conservative, i.e. resulting in a larger d_{SB}; higher values of SF (up to 2) can be used after it is confirmed (e.g. by visual observations) that the damage occurred on the opposite sides of the tunnel
- d_{SB}/L_d = 0.05, representing a reasonable distribution of stress fracturing along the tunnel, as observed in several hard rock mines.

This yields the following cubic equation for d_{SB}:

$$d_{SB}^3 + D d_{SB}^2 - 0.676 t_{SB} \rho\beta^3 R\, PGD/\sigma_{1p} = 0 \quad (3)$$

which can be solved numerically or approximated by $d_{SB} \approx d_0 + d_1$, where $d_0 = \sqrt{0.676 t_{SB} \rho \beta^3 R\, PGD / (\sigma_{1p} D)}$ and $d_1 = -d_0^2/(2D + 3d_0)$.

The bulking (strainburst) velocity can then be calculated using the BF:

$$V_{SB} = BF\, d_{SB}/t_{SB} \tag{4}$$

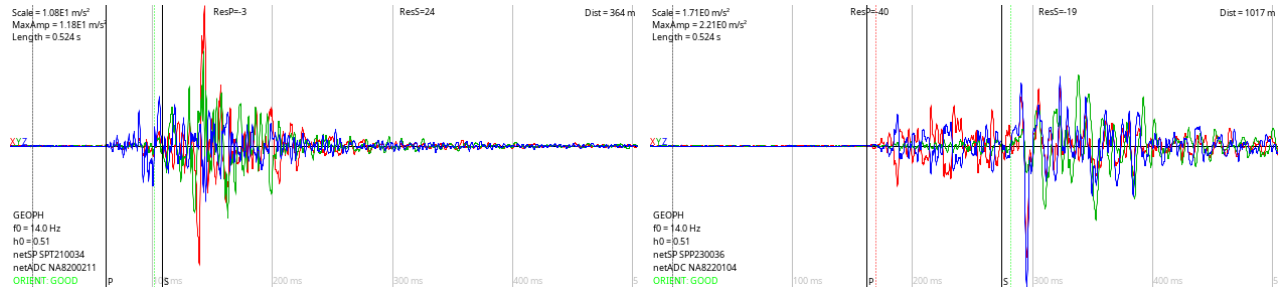
3 Example A

A moment magnitude M_W2.5 event that occurred at a hard rock mine is analysed in this section. The recorded waveforms consisted of multiple pulses. One example is shown in Figure 2a. The initial pulse, which was used to locate the source initiation, had an amplitude approximately 10-times smaller than the pulses recorded 15–20 ms later.

The seismic source mechanism inferred from the low-frequency radiation (including all pulses) was slip-type; therefore, the McGarr (1991) method was applied. The acceleration waveforms were low-pass filtered at 100 Hz and used to measure the peak amplitude a. Two examples are shown in Figure 5.

The reason for applying a 100 Hz low-pass filter is that ground motion at higher frequencies is ineffective at producing relative displacement between supported blocks of rock and the surrounding rock mass, as discussed by Malovichko & Kaiser (2020).

The near-source PGV (equal to $\dot{D}/2$) was evaluated at the six nearest monitoring sites, yielding a median value of 1.29 m/s. The following parameters were used: rock mass density ρ = 2,700 kg/m^3, S-wave velocity β = 3,406 m/s, and shear modulus μ = 31 GPa.



(a) (b)

Figure 5 Acceleration waveforms of the M_W2.5 event, corrected for the instrument response and low-pass filtered at 100 Hz. The details and results of the maximum near-source ground velocity ($\dot{D}/2$) evaluation are shown below each waveform. (a) a = 11.8 m/s^2, R = 364 m, $\dot{D}/2$ = 1.67 m/s; (b) a = 2.21 m/s^2, R = 1017 m, $\dot{D}/2$ = 0.92 m/s

The next step was to produce a map of the dynamic demand. The source was approximated by the ellipsoid shown in Figure 6 based on the following observations:

- The location of the mainshock initiation and its associated uncertainty
- The mechanism of the mainshock
- The locations and mechanisms of the aftershocks recorded within one hour of the mainshock.

The dynamic demand map, expressed in terms of PGV, was then calculated using the GMPE calibrated for the mine, with the near-source PGV term adjusted to 1.29 m/s. The results are presented in Figure 6.

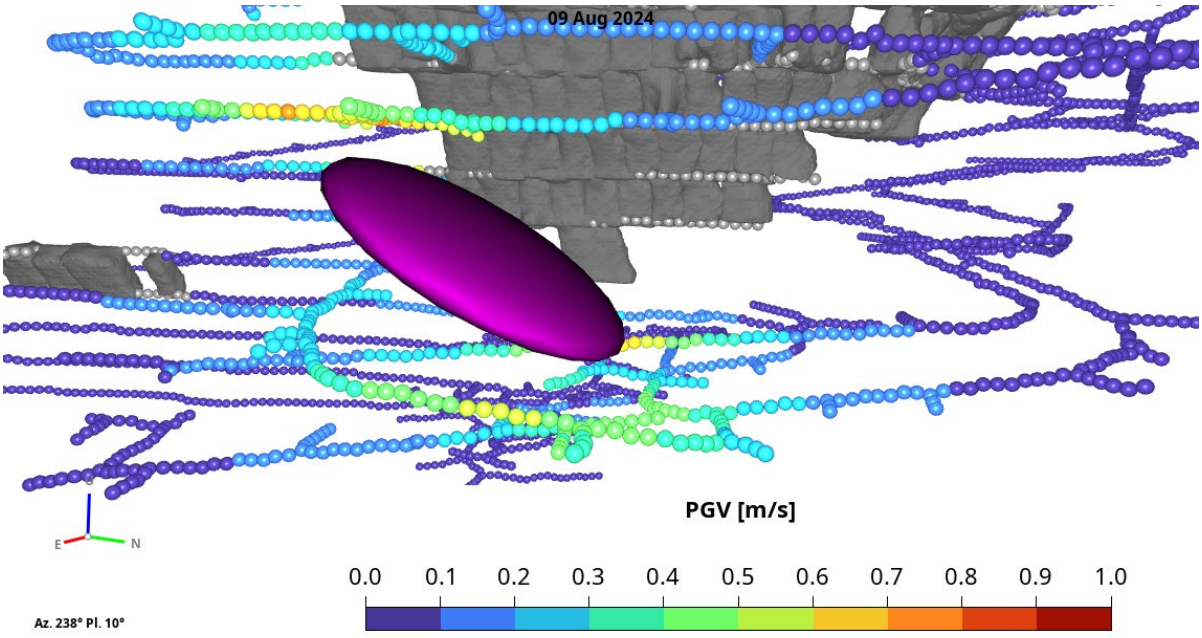


Figure 6 Approximation of the M_W2.5 event source (magenta ellipsoid) and peak ground velocity evaluated for the nearby tunnels

4 Example B

This section discusses a moment magnitude M_W2.6 event that occurred at another hard rock open-stoping mine. Similar to the previous case, the recorded waveforms were complex, with weaker initial P-wave and S-wave arrivals followed by stronger later signals. One example is shown in Figure 2b.

The source initiation was located near the ore drives, and the 95% confidence region for its location intersected the orebody. The seismic source mechanism inferred from the low-frequency radiation was crush-type, with the P-axis oriented approximately perpendicular to the orebody. The source was therefore interpreted as a sequence of episodes of sudden stress-induced fracturing on the backs and/or floors of the ore drives and, possibly, along the stope perimeters.

A conservative evaluation of the demand in terms of d_{SB} and V_{SB} can be performed using the procedure described in the second part of Section 2, assuming that the most intense phase of seismic radiation originated from the ore drives rather than the stopes. The application of the procedure to 2 representative waveforms is illustrated in Figure 7. The following parameters were used: rock mass density ρ = 2,700 kg/m^3, S-wave velocity β = 3,700 m/s, maximum in-plane stress σ_{1p} = 80 MPa, effective tunnel diameter = 6 m, BF = 3%.

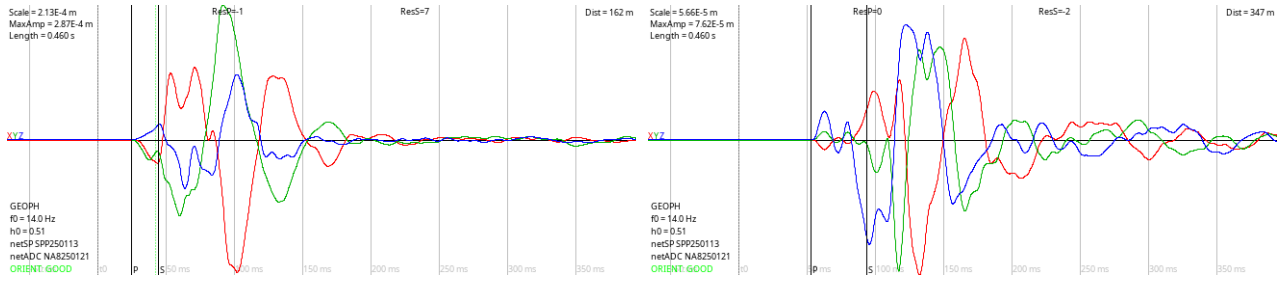


Figure 7 Displacement waveforms of the M_W2.6 event. The details and results of the maximum strainburst depth (d_{SB}) and bulking velocity (V_{SB}) evaluation are shown below each waveform. (a) PGD = 2.87·10^{-4} m, R = 162 m, t_{SB} = 32 ms, d_{SB} = 10.6 m, V_{SB} = 9.9 m/s; (b) PGD =7.62·10^{-5} m, R = 347 m, t_{SB} = 35 ms, d_{SB} = 8.57 m, V_{SB} = 7.3m/s

The median values of d_{SB} and V_{SB} based on the measurements at the 7 nearest sites are 8.1 m and 6.9 m/s, correspondingly.

Based on the uncertainty of source initiation location and stress conditions of the tunnels, the source volume was established as shown by ellipsoid in Figure 8. It was conservatively assumed that the evaluated median values of d_{SB} and V_{SB} could be attributed to the tunnels within this volume. The cosine shape of the spatial distribution of d_{SB} along tunnels from Malovichko (2022) was used with the default shape factor d_{SB}/L_d = 0.05 discussed in Section 2. The resulting map of the demand parameters is presented in Figure 8.

The obtained d_{SB} and V_{SB} values appear to be extreme. One possible explanation is that the largest pulse in the displacement waveforms is associated with failure at the perimeter of the stopes or even of a pillar between the stopes. In such a case, the extent and rate of stress fracturing around the tunnels could be much smaller than those shown in Figure 8. Therefore, the resulting d_{SB} and V_{SB} maps represent a worst-case interpretation of the recorded seismic radiation. Such an interpretation can be useful in an operational context.

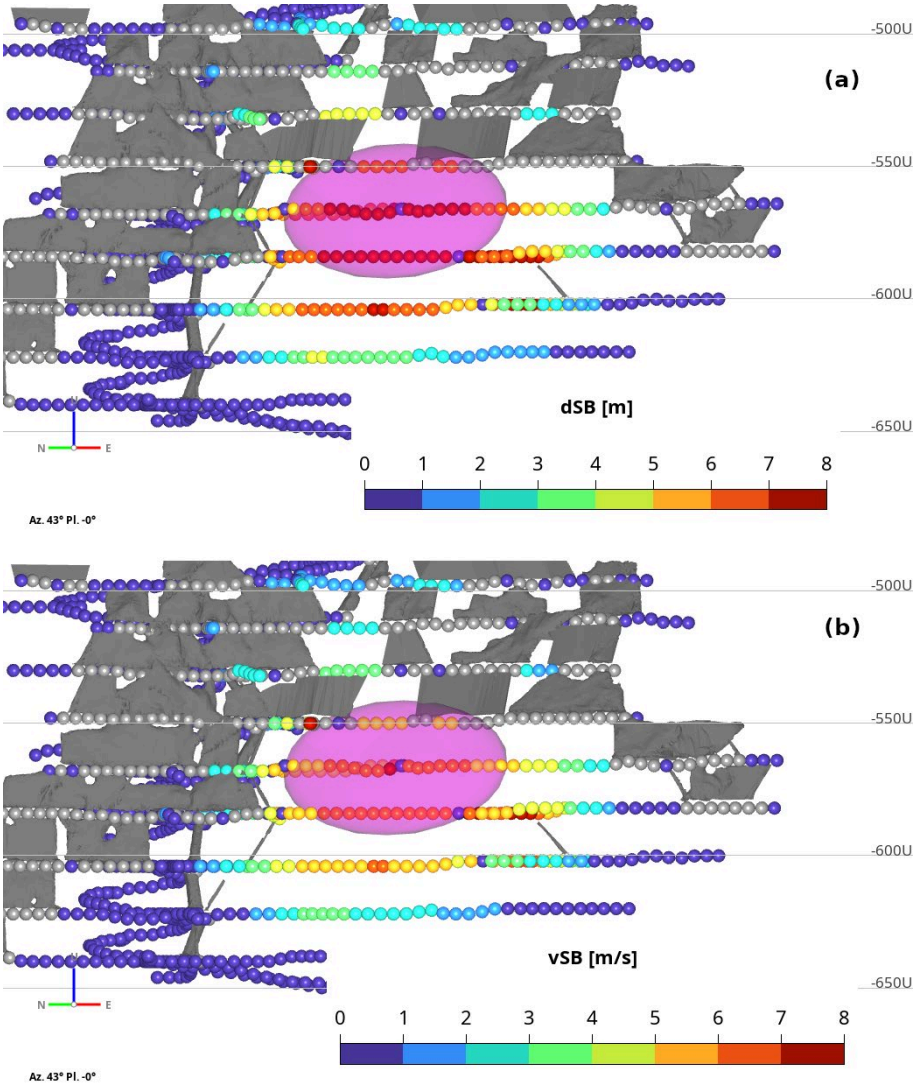


Figure 8 Approximation of the M_W2.6 event source (magenta ellipsoid) and express evaluation of dynamic demand parameters for the nearby tunnels. (a) Strainburst depth (d_{SB}); (b) Bulking velocity (V_{SB})

5 Discussion and conclusions

The presented examples illustrate that the proposed calculations of dynamic demand parameters for large, complex seismic events are relatively simple and can be completed within an hour after the event. However, it is important to keep in mind that they represent a highly conservative, approximate assessment and should ideally be followed by a more accurate, albeit more time-consuming, evaluation based on finite-source inversion.

A possible application of the proposed demand calculations is the reconnaissance assessment of damage likelihood. This requires information about the installed ground support, specifically its remnant capacity in terms of displacement and energy. To illustrate such an assessment, we consider 3 generic support types:

- Light: rebar with 1.5 m x1.5 m spacing + 50 mm fibre reinforced shotcrete (FRS).
- Standard: rebar with 1.1 m x 1.1 m spacing + 50 mm FRS + 4GA mesh.
- Heavy: Posimix with 1.1 m x 1.1 m + cable bolt with 1.5 m x 1.5 m spacing + 50 mm FRS + 4GA mesh.

The methodology for comparing strainburst and shakedown demand with ground support capacity in terms of displacement and kinetic energy can be found in (Rigby et al. 2026a, 2026c).

In Example A, the demand is moderate and is expected to cause damage to the areal support in the case of the light support system, as shown in Figure 9. The inertia of wedges between the rockbolts, accelerated by the ground motion associated with the event, is sufficient to fracture the 50 mm FRS in multiple tunnels.

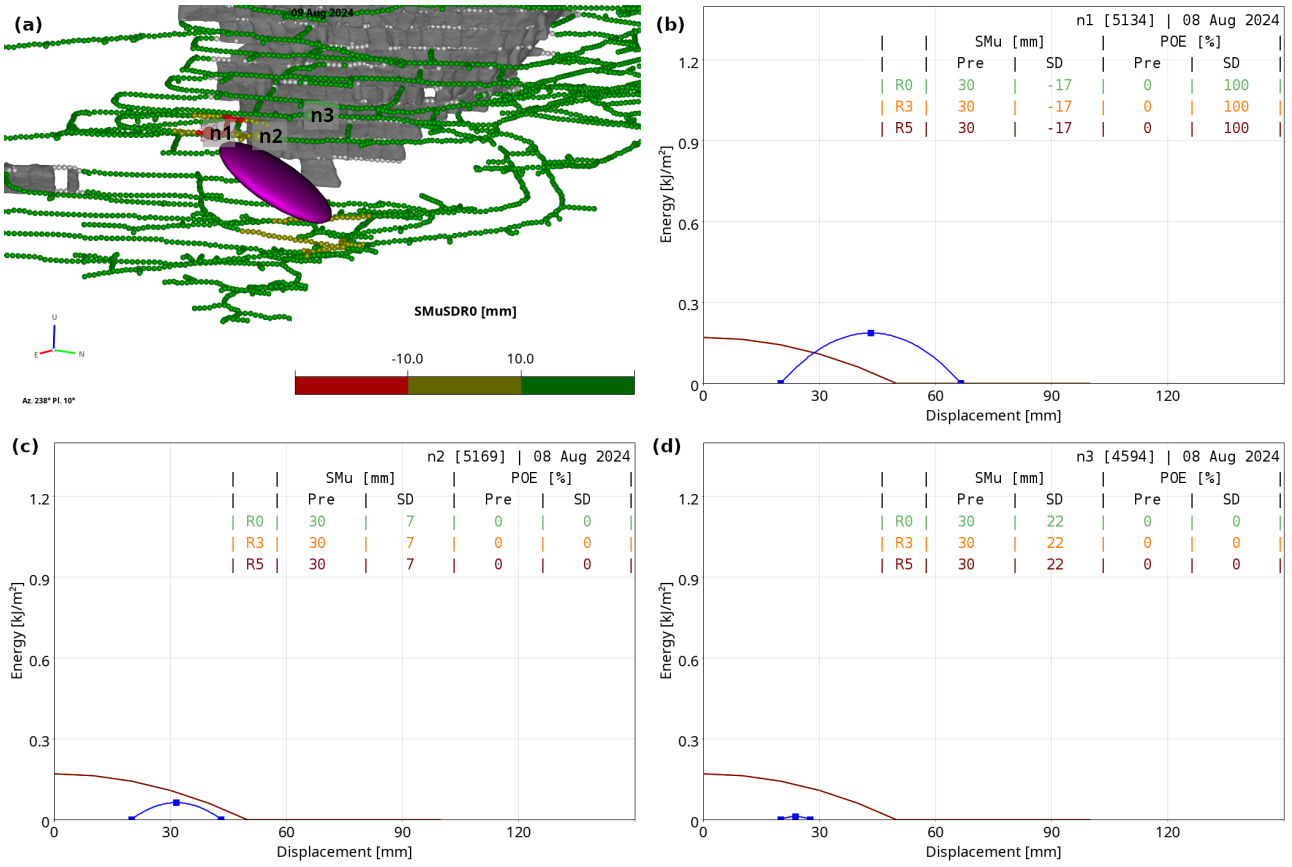


Figure 9 (a) Displacement safety margin (SMu) for light (R0) shakedown damage based on the demand estimated from the peak ground velocity map shown in Figure 6 and the light ground support; Examples of SMu calculations for the three charateristic locations marked in the map: (b) n1, (c) n2 and (d) n3. The brown line represents the remnant capacity of the areal support, while the blue trajectories describe the shakedown demand

If a heavy ground support system is assumed for the same event, no damage is expected (Figure 10). The PGV is relatively low and should cause only minimal yielding (a few millimetres) of the rockbolts and areal support.

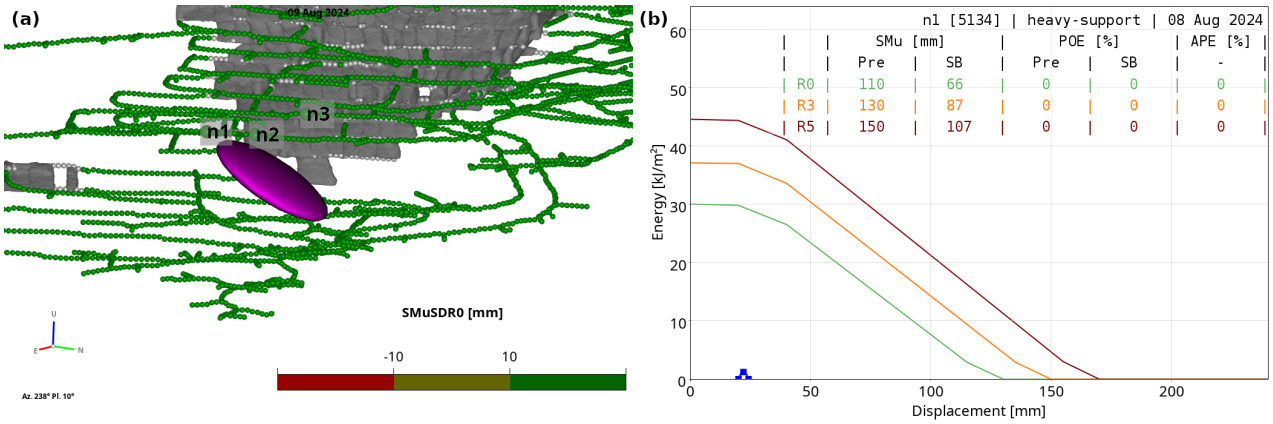


Figure 10 (a) Displacement safety margin (SMu) for light (R0) shakedown damage based on the demand estimated from the peak ground velocity (PGV) map shown in Figure 6 and the heavy ground support; (b) Details of SMu calculation for the charateristic location n1 with the maximum PGV. The green, yellow and red lines represent the remnant capacity of the support for light, moderate and severe damage, correcpondingly. The blue trajectory describes the shakedown demand

In Example B, the demand is significant, and severe damage is expected. Figure 11 shows the results of the performance assessment for the standard support system.

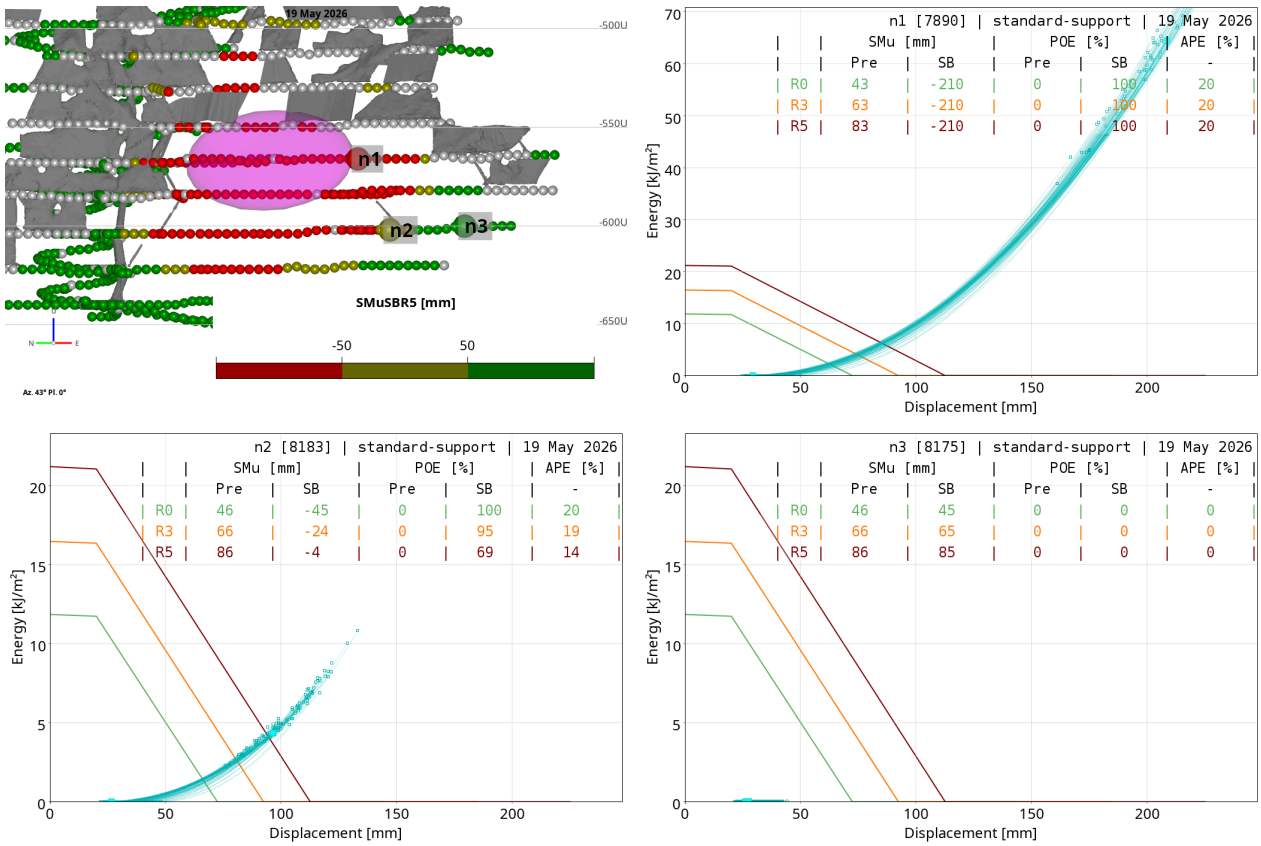


Figure 11 Displacement safety margin (SMu) for severe (R5) strainburst damage based on the demand estimated from the strainburst depth (d_{SB}) and bulking velocity (V_{SB}) maps shown in Figure 8 and the standard ground support (top left). Examples of SMu calculations for the 3 characteristic locations marked in the map

The presented results illustrate that the likelihood of damage, accounting for both the dynamic demand and the characteristics of the ground support, can be evaluated in an operational context.

The proposed approach has several limitations that warrant further work:

- Some large crush-type events involve a combination of failure at the perimeter of large-scale excavations (e.g. stopes or caves) and stress-induced fracturing around tunnels, as illustrated in Figure 12. Consequently, the strongest radiation pulse may not be associated with a particular tunnel, and the values of d_{SB} and V_{SB} obtained using the procedure described in Section 2 may be overestimated. This is most likely what occurred in Example B. A reasonable partitioning of the recorded seismic radiation between tunnels and larger-scale excavations would improve the demand assessment and is one of the highest priorities for future development of the method.
- This paper considers 2 types of dynamic demand imposed on ground support. The first is driven by seismic waves generated by external failure (typically slip-type or shear-type failure), while the second is caused by dynamic stress fracturing at the tunnel perimeter and the subsequent bulking of the fractured rock. However, other loading mechanisms also exist. For example, geological structures in the immediate vicinity of tunnels may amplify stress fracturing, giving rise to what is referred to as structurally controlled strainburst. The corresponding seismic radiation is characterised by a combination of slip- and crush-type source mechanisms (Rigby et al. 2026b). In addition, even moderate PGV generated by a slip-type event may trigger strainbursting in a highly stressed tunnel excavated in brittle rock. Therefore, it would be beneficial to account for these rockburst damage mechanisms when assessing the dynamic demand.

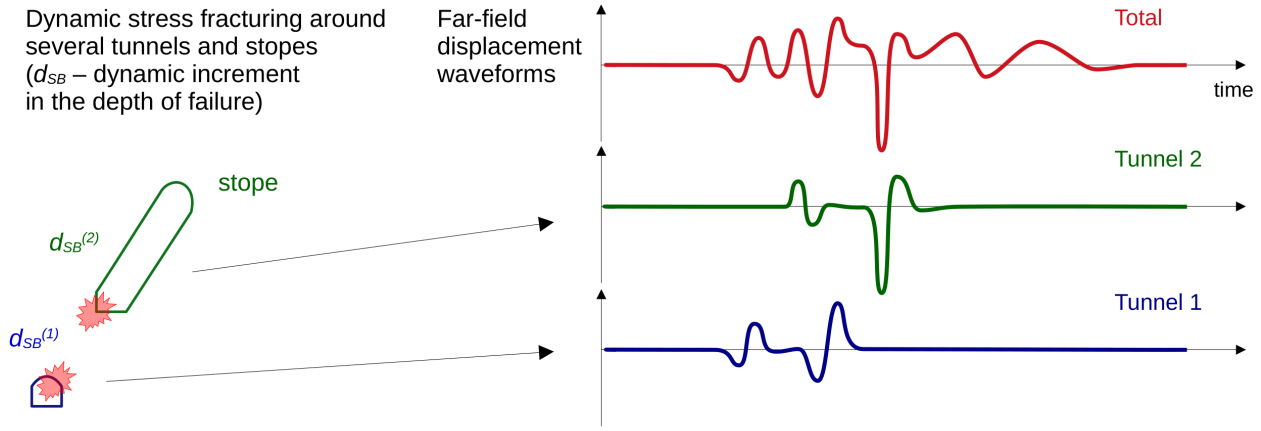


Figure 12 Hybrid crush-type event involving dynamic stress fracturing around stope and tunnels. d_{SB} = strainburst depth

The main conclusions are as follows:

- When evaluating the dynamic demand imposed on ground support, it is important to account for differences in seismic source mechanisms and ground support loading processes. The presented examples illustrate that events of similar magnitude may produce substantially different demand in terms of the velocity of the ground around or within the supported rock (compare the PGV and V_{SB} values in Figures 6 and 8).
- The proposed conservative express evaluation of the demand can be completed within an hour after the event.
- The estimated demand, in terms of both strainburst and shakedown damage mechanisms, can be compared with the ground support capacity to assess the likelihood of damage.

Acknowledgement

The permission granted by the participating mines to present the real data is gratefully appreciated.

References

Kaiser, P, McCreath, D & Tannant, D 1996, *Canadian Rockburst Support Handbook*, Mining Research Directorate, Sudbury, https://www.geo-kaiser.ca

Kaiser, P K & Malovichko, D A 2022, 'Energy and displacement demands imposed on rock support by strainburst damage mechanisms', in M Diederichs (ed), *Proceedings of the 10th International Symposium on Rockbursts and Seismicity in Mines (RaSiM11)*, Society for Mining, Metallurgy & Exploration, Englewood.

Malovichko, D 2022, 'Keynote: utility of seismic source mechanisms in mining', in M Diederichs (ed), *Proceedings of the 10th International Symposium on Rockbursts and Seismicity in Mines (RaSiM11)*, Society for Mining, Metallurgy & Exploration, Englewood.

Malovichko, D & Kaiser, PK 2020, 'Dynamic model for seismic shakedown analysis', *Proceedings of the 54th US Rock Mechanics/Geomechanics Symposium*, American Rock Mechanics Association, Eaton.

Malovichko, DA & Rigby, A 2022, 'Description of seismic sources in underground mines: dynamic stress fracturing around tunnels and strainbursting', *arXiv preprint*, https://doi.org/10.48550/arXiv.2205.07379

Malovichko, D, Rigby, A, Jessu, K & Viegas, G 2024, 'Forecasting shaking and bulking ground velocities around tunnels for a planned mining sequence', in P Andrieux & D Cumming-Potvin (eds), *Deep Mining 2024: Proceedings of the 10th International Conference on Deep and High Stress Mining*, Australian Centre for Geomechanics, Perth, pp. 687–698, https://doi.org/10.36487/ACG_repo/2465_42

Malovichko, D, Jaimes, A & Lotter E C 2025, 'Finite seismic sources in mines: Inversion and utilisation', in S Dineva (ed.), *Proceedings of the 11th International Symposium on Rockbursts and Seismicity in Mines (RaSiM11)*, Luleå University of Technology, Luleå, pp. 260–286.

McGarr, A 1991, 'Observations constraining near-source ground motion estimated from locally recorded seismograms', *Journal of Geophysical Research*, vol. 96, no. B10, pp. 16495–16508.

Mendecki, A J 2019, 'Simple GMPE for underground mines', *Acta Geophysica*, vol. 67, pp. 837–847.

Rigby, A, Malovichko, D & Kaiser PK 2026a, 'A rockburst hazard assessment framework for strainbursting', *Rock Mechanics and Rock Engineering*, https://doi.org/10.1007/s00603-026-05461-8

Rigby, A, Malovichko, D & Kaiser PK 2026b, 'Modelling the effect of geological structures on strainburst dynamics and associated seismic radiation pattern', *Proceedings of the Australian Conference on Rock Mechanics 2026*, Australian Geomechanics Society, Melbourne.

Rigby, A, Malovichko, D & Kaiser PK 2026c, 'Modelling shakedown demand on ground support', in D Cumming-Potvin & J Wesseloo (eds), *Ground Support 2026: Proceedings of the 11th International Conference on Ground Support in Mining*, Australian Centre for Geomechanics, Perth, https://doi.org/10.36487/ACG_repo/2625_44